Supplementary Information

Effects of spin-phonon coupling on two-dimensional ferromagnetic

semiconductors: a case study of iron and ruthenium trihalides

Yinqiao Liu[1], Qinxi Liu[1], Ying Liu[1], Xue Jiang[1,*], Xiaoliang Zhang[2], Jijun Zhao[1]

[1]Key Laboratory of Material Modification by Laser, Ion and Electron Beams (Dalian University of Technology), Ministry of Education, Dalian 116024, China

[2]Key Laboratory of Ocean Energy Utilization and Energy Conservation of Ministry of Education, School of Energy and Power Engineering, Dalian University of Technology, Dalian 116024, China.

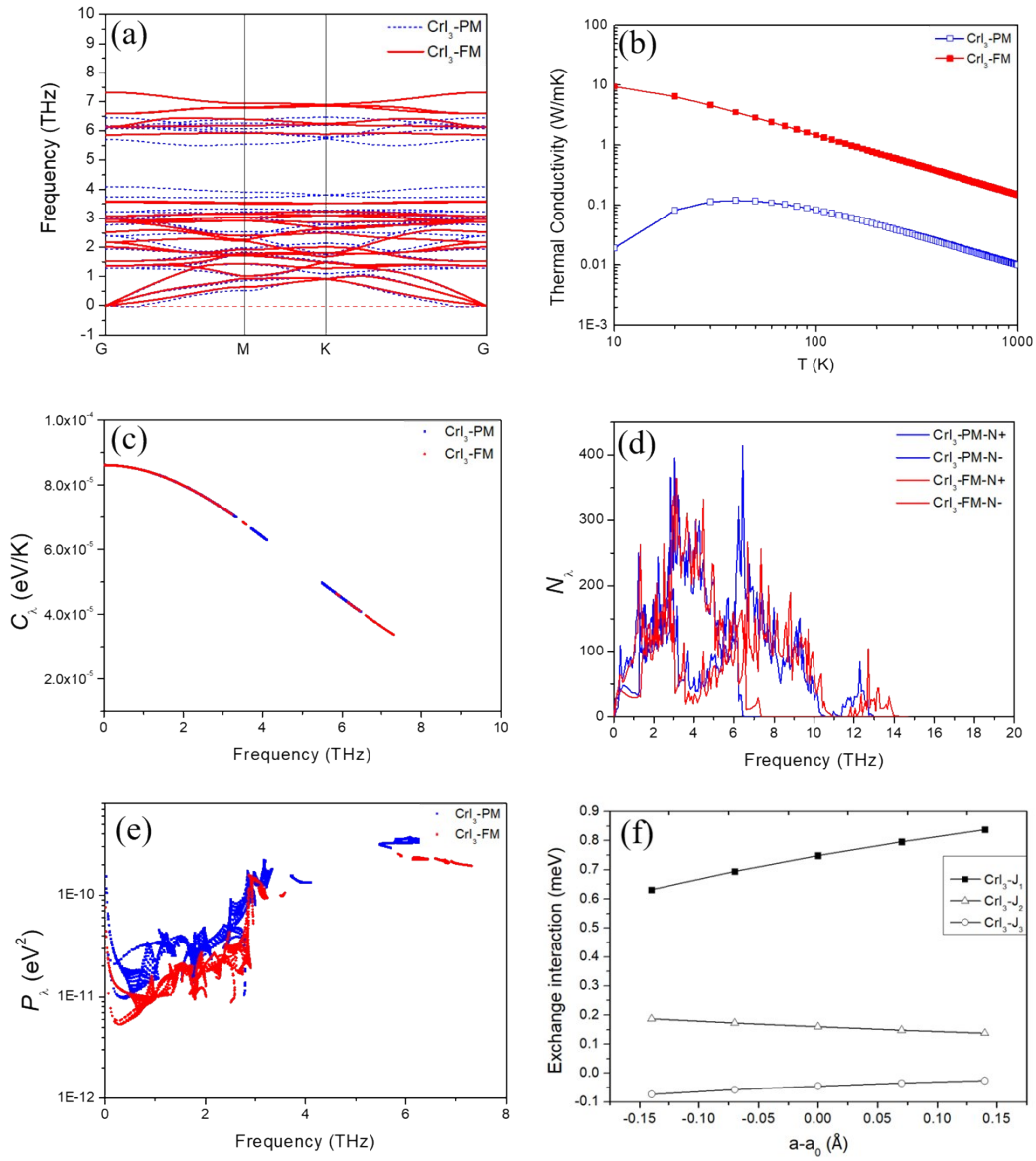*Corresponding author. E-mail: jiangx@dlut.edu.cn (Xue Jiang)

FIGURE S1. Effects of SPC on various phonon-related properties of monolayer CrI₃: (a) phonon dispersion curve; (b) lattice thermal conductivity; (c) mode dependent heat capacity; (d) scattering possibility; (e) phonon interaction strength; and (f) dependence of magnetic-exchange interaction parameters on lattice constant.
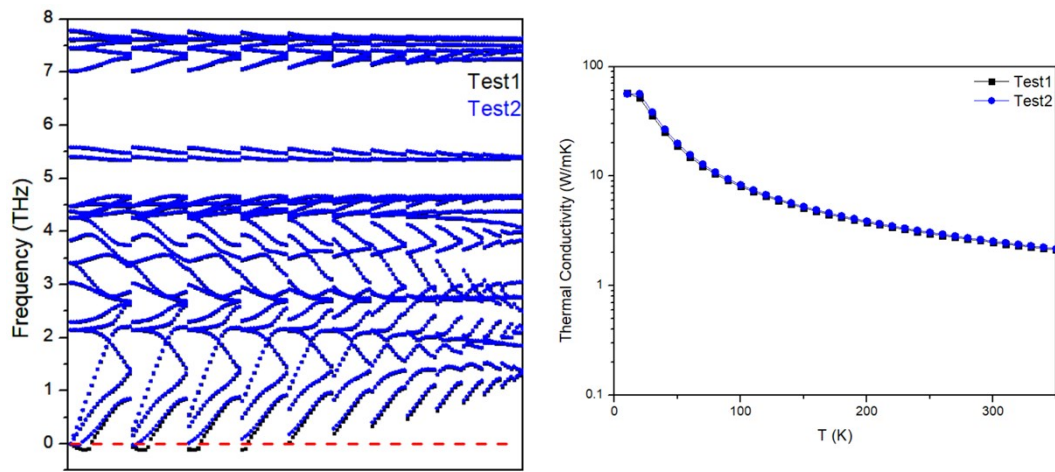
FIGURE S2. (Left) Phonon dispersion data of full reciprocal space. The small imaginary frequency of PM-FeBr$_3$ will disappear by enlarge the size of the supercell, e.g. from test1 to test2. (Right) Small imaginary frequency nearly unchanged the lattice thermal conductivity of PM-FeBr$_3$.
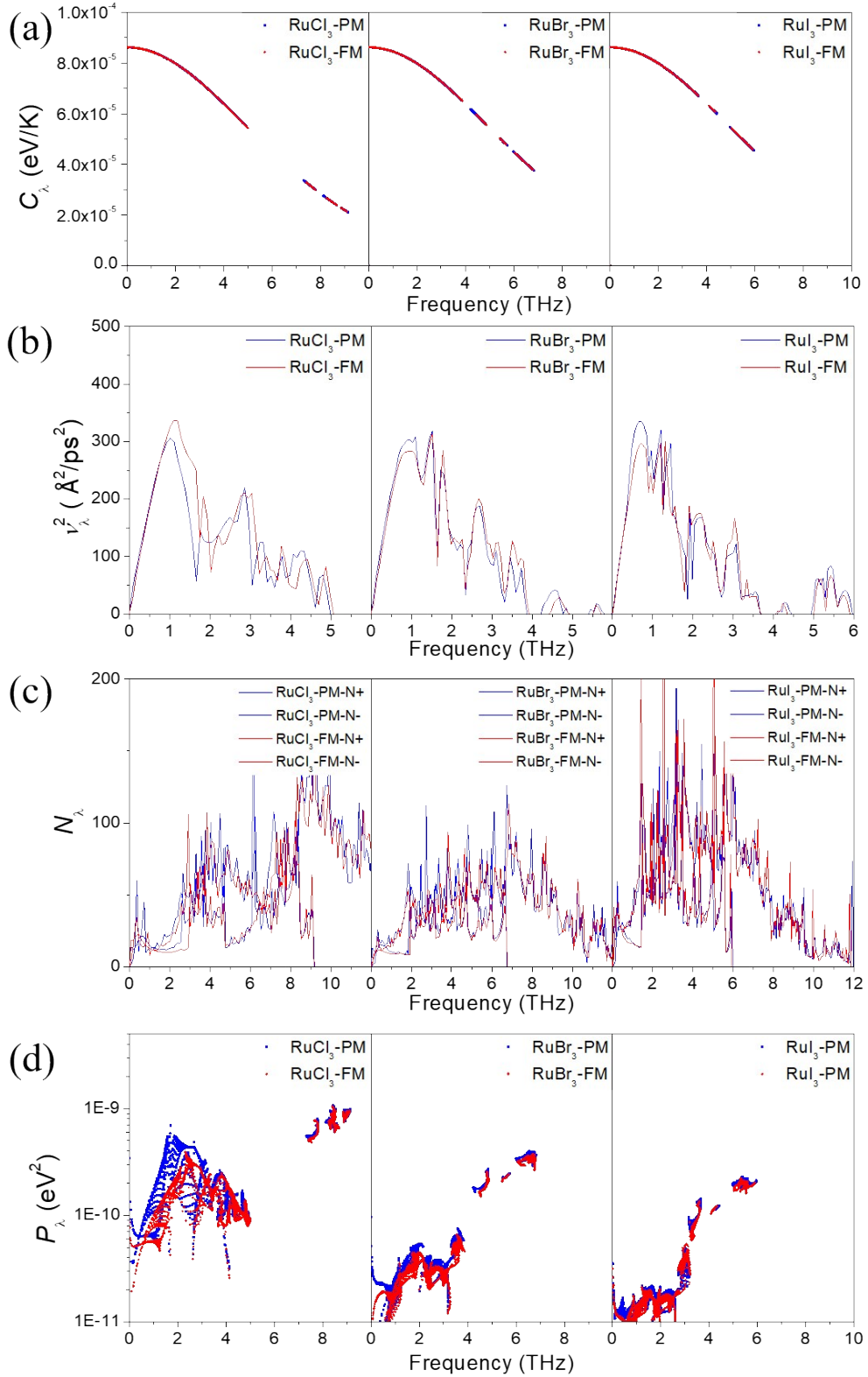
FIGURE S3. Effects of SPC on (a) mode dependent heat capacity, (b) production of group velocities, (c) scattering possibility, and (d) average phonon–phonon interaction strength for $RuCl_3$, $RuBr_3$, and RuI_3, respectively.
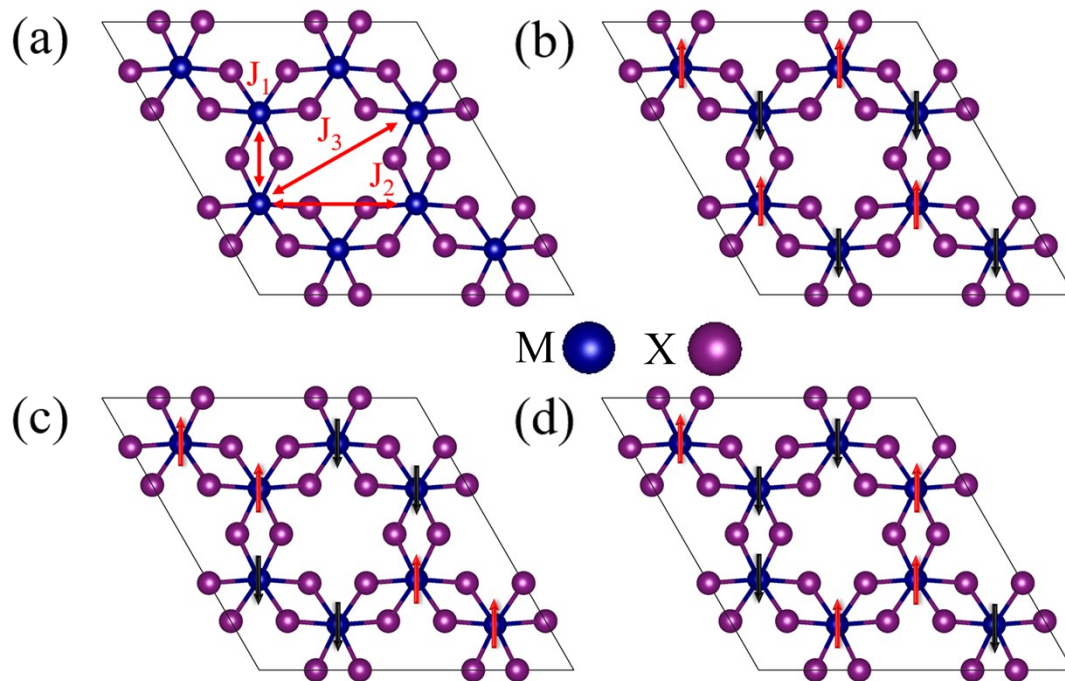
FIGURE S4. (a) Top view of MX_3 monolayers. Considered exchange paths are shown by red double arrows. Possible antiferromagnetic (AFM) magnetic configurations of MX_3 monolayers with: (b) Néel-AFM, (c) stripy-AFM, and (d) zigzag-AFM orderings.

FIGURE S5. Curie temperatures with or without lattice deformation, C is heat capacity.
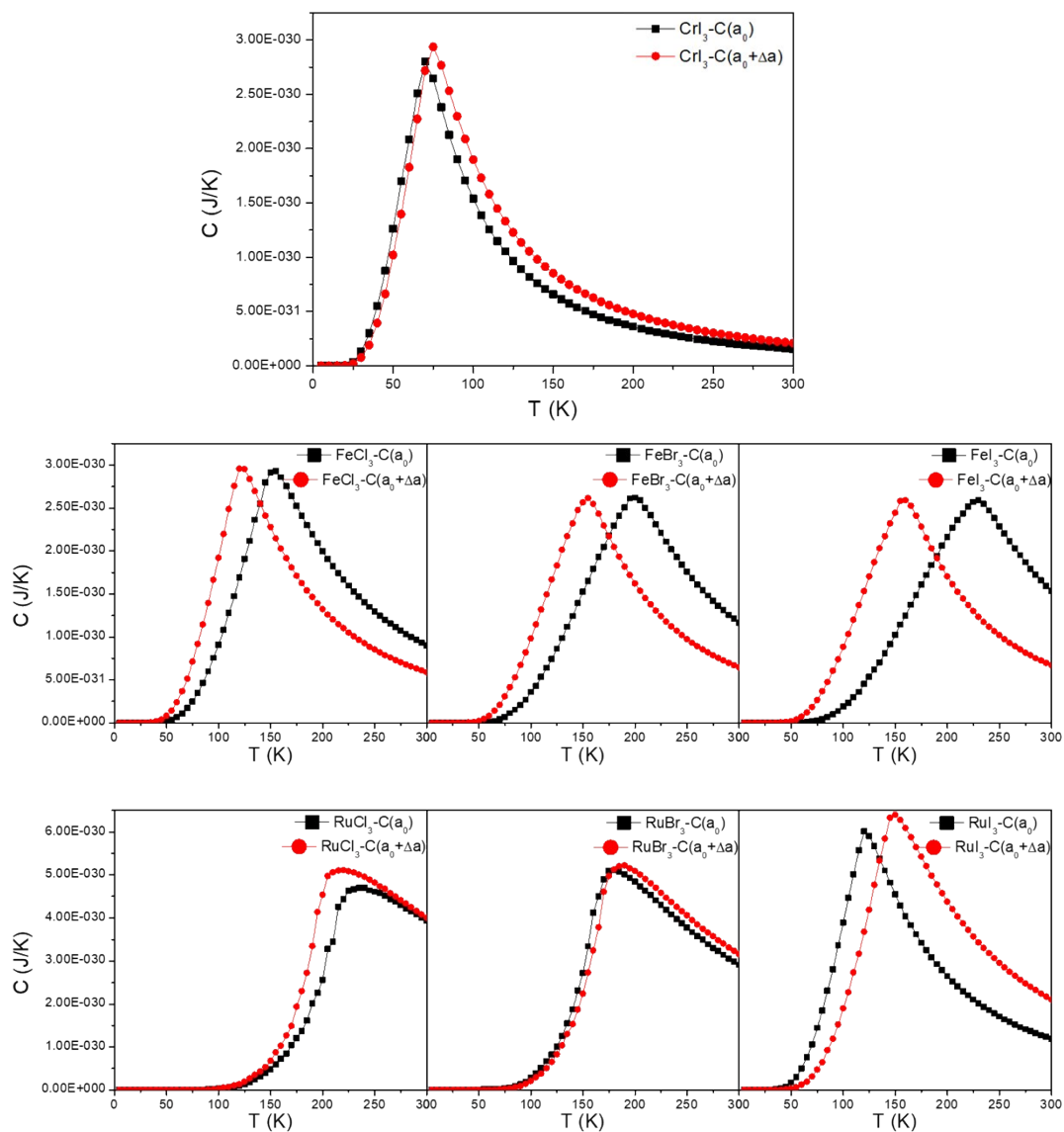
TABLE S1. The difference in the total energy per unit cell between the FM, PM states $(E_{\mathrm{FM}}-E_{\mathrm{PM}})$ or FM, antiferromagnetic (AFM) states $(E_{\mathrm{AFM}}-E_{\mathrm{FM}})$, respectively.

	$FeCl_3$	$FeBr_3$	FeI_3	$RuCl_3$	$RuBr_3$	RuI_3	CrI_3	VCl_3	VBr_3	VI_3
$E_{\mathrm{FM}}-E_{\mathrm{PM}}$ [eV]	−1.064	−1.024	−0.543	−0.195	−0.136	−0.045	−3.374	−1.265	−1.406	−1.509
$E_{\mathrm{AFM}}-E_{\mathrm{FM}}$ [eV]	−0.073	−0.058	−0.061	0.199	0.153	0.069	0.037	−	−	−

TABLE S2. The total energy per unit cell of AFM states.

Energy [eV]	FM	Néel-AFM	stripy-AFM	zigzag-AFM
CrI_3	−31.838	−31.802	−31.801	−31.816
$FeBr_3$	−29.906	−29.965	−29.971	−29.964
$FeCl_3$	−33.289	−33.363	−33.359	−33.338
FeI_3	−26.576	−26.637	−26.672	−26.666
$RuBr_3$	−30.500	−30.347	−30.409	−30.449
$RuCl_3$	−33.525	−33.326	−33.400	−33.435
RuI_3	−28.196	−28.127	−28.136	−28.162

TABLE S3. Magnetic moment M and exchange parameters J (in meV).

	M [μB]	J1	J2	J3	M(strain =10%)	J1(strain =10%)	J2(strain =10%)	J3(strain =10%)
CrI$_3$	3.02	0.590	0.080	0.213	3.05	0.692	0.053	0.178
FeBr$_3$	3.72	−0.913	0.212	−0.130	3.74	−0.696	0.163	−0.107
FeCl$_3$	3.80	−0.916	0.069	−0.141	3.82	−0.742	0.049	−0.116
FeI$_3$	3.56	−1.091	0.285	−0.404	3.58	−0.756	0.193	−0.342
RuBr$_3$	0.73	52.648	−5.263	−5.341	0.75	54.326	−5.727	−5.156
RuCl$_3$	0.82	61.396	−7.271	−11.736	0.82	62.859	−8.427	−12.306
RuI$_3$	0.67	23.928	1.489	4.541	0.69	31.742	0.467	3.450